

Mathematical method for designing superresolution lenses using superoscillations

MATT K. SMITH AND GREG GBUR* 

Department of Physics and Optical Science, The University of North Carolina at Charlotte, Charlotte, North Carolina 28223, USA

*Corresponding author: gjgbur@uncc.edu

Received 27 January 2020; revised 19 February 2020; accepted 20 February 2020; posted 20 February 2020 (Doc. ID 388252); published 20 March 2020

We use a new mathematical method to design a superresolution lens using a superoscillation technique based on polynomial roots. We walk through an example of the method using simulations. Our method allows for ease of design by being mathematically and conceptually simpler than other methods. © 2020 Optical Society of America

<https://doi.org/10.1364/OL.388252>

Resolution better than that allowed by the diffraction limit, called superresolution, is an important strategy for improving the performance of optical systems. Although there is no unique definition of resolution, it is intimately related to the width of the system's point spread function (PSF); for a single thin lens, the PSF is the well-known Airy disk. The Rayleigh criterion defines the resolution of a lens as the distance from the center of the PSF's central lobe to the first zero ring of the PSF. A number of different methods for attaining superresolution have been introduced, including lens coatings [1,2], structured illumination [3], and near-field imaging [4].

One superresolution method introduced in recent years employs so-called superoscillations—oscillations in a band limited signal that are faster than the band limit would seem to permit [5,6]. These oscillations, which may be interpreted as a delicate interference phenomenon, are not restricted to the near-field of an imaging system. The first use of a superoscillatory lens (SOL) to achieve superresolution was developed by Huang and Zheludev [7]. They used prolate spheroidal wavefunctions to design an intensity and phase modulating mask to produce a one-dimensional super-oscillatory region in the image plane. Rogers *et al.* later introduced an SOL with a binary mask [8], simplifying the lens design. SOLs have also been developed using optical eigenmodes [9], and achromatic SOLs have been introduced [10] to reduce wavelength sensitivity.

One consistent challenge in applying superoscillations in optics is the rather complicated mathematics often used, such as asymptotic analysis [5] or Tschebyscheff polynomials [11]. Recently, however, an intuitive strategy for designing super-oscillatory functions was introduced by Chremmos and Fikioris [12] based on the straightforward application of polynomials and their zeros. This one-dimensional method was later expanded to two dimensions and shown to be able to produce

superoscillatory patterns of optical vortices by the current authors [13].

In this Letter, we modify the polynomial superoscillation methods from Refs. [12,13] to create a new method for designing SOLs and demonstrate its performance with simulations. We go through the entire process of designing a superresolution lens and discuss some advantages and drawbacks of our method.

First, we will briefly review the polynomial method from Ref. [13]. Suppose we have a two-dimensional (2D) function $t(x, y)$, whose Fourier transform $\tilde{t}(k_x, k_y)$ is band limited to the range $k_x^2 + k_y^2 \leq k_{\max}^2$. This function will generally not have any oscillations with a wavelength smaller than $\lambda_{\min} = 2\pi/k_{\max}$. We now multiply $t(x, y)$ by a complex polynomial $h(x, y)$, defined as

$$h(x) := \prod_{n=1}^N (\bar{z} - \bar{z}_n), \quad (1)$$

where N is the order of the polynomial, $\bar{z} = x + iy$, and \bar{z}_n are the complex zeros of the polynomial. We label the product as $s(x, y) := h(x, y)t(x, y)$. If two or more zeros are spaced closer than $\lambda_{\min}/2$, then locally the field is oscillating faster than conventional Fourier theory allows; it is superoscillatory [5].

We note that multiplying $t(x, y)$ by $h(x, y)$ does not change the band limit. This is because the polynomial terms in $h(x, y)$ convert to derivatives in the Fourier transform operation. That is, if we rewrite $h(x, y)$ as

$$h(x, y) = \sum_{n=0}^N c_n \bar{z}^n, \quad (2)$$

where c_n are complex constants, then the Fourier transform of $s(x, y)$ may be written as

$$\tilde{s}(k_x, k_y) = \sum_{n=0}^N i^n c_n \left(\frac{\partial}{\partial k_x} + i \frac{\partial}{\partial k_y} \right)^n \tilde{t}(k_x, k_y). \quad (3)$$

The function $\tilde{s}(k_x, k_y)$ has the same band limit as $\tilde{t}(k_x, k_y)$ since the derivatives will be identically zero outside the band limit. We also note that Eq. (3) indicates that the first $N - 1$ derivatives of $\tilde{t}(k_x, k_y)$ must be continuous to avoid having Dirac delta singularities in $\tilde{s}(k_x, k_y)$ [13].

The method described above only produces zeros at isolated *points* in the xy plane; for superresolution imaging, we desire zero *rings* to limit the radius of the PSF. Modifying our approach to achieve this is the focus of this Letter.

In Fig. 1, we show an arrangement for superresolution imaging with an SOL. The SOL consists of a lens contained within an aperture, preceded by a transmission mask. We assume that light from a point-like source in the object plane propagates along the z axis and that the mask has a transmission function $t(\mathbf{r}_L)$. We take the object and image distances to be d_o and d_I , respectively, so that the field $U_I(\mathbf{r}_I)$ in the image plane has the well-known form

$$U_I(\mathbf{r}_I) = \frac{iU_0 e^{ik_0 d_I}}{\lambda_0 d_I} e^{\frac{ik_0}{2} \left(\frac{|\mathbf{r}_o|^2}{d_o} + \frac{|\mathbf{r}_I|^2}{d_I} \right)} \times \iint_A t(\mathbf{r}_L) e^{-ik_0 \left(\frac{r_o}{d_o} + \frac{r_I}{d_I} \right) \cdot \mathbf{r}_L} d^2 \mathbf{r}_L. \quad (4)$$

Here, U_0 is the object-field amplitude, λ_0 is the wavelength, $k_0 = 2\pi/\lambda_0$, A is the aperture area, and \mathbf{r}_o , \mathbf{r}_I , and \mathbf{r}_L are the xy coordinate vectors for the object, image, and lens planes, respectively. We note that Eq. (4) depends on the Fourier transform of the transmission function, i.e.,

$$U_I(\mathbf{r}_I) = \gamma(\mathbf{r}_I, \mathbf{r}_o) \iint_A t(\mathbf{r}_L) e^{-i\mathbf{k}(\mathbf{r}_o, \mathbf{r}_I) \cdot \mathbf{r}_L} d^2 \mathbf{r}_L, \quad (5)$$

where $\gamma(\mathbf{r}_I, \mathbf{r}_o)$ contains all the functions and constants in front of the integral in Eq. (4), and $\mathbf{k}(\mathbf{r}_o, \mathbf{r}_I)$ is defined as

$$\mathbf{k}(\mathbf{r}_o, \mathbf{r}_I) := k_0 \left(\frac{\mathbf{r}_o}{d_o} + \frac{\mathbf{r}_I}{d_I} \right). \quad (6)$$

With Eq. (5), we can now see how the polynomial method can be used to design an SOL. The field in the image plane is proportional to the Fourier transform of the transmission function $t(\mathbf{r}_L)$. If we have a circular aperture and no transmission mask, the system will produce the classic lens PSF, an Airy disk, with a first zero ring at radius Δ_{UL} ,

$$\Delta_{UL} = \frac{3.83 d_I \lambda_0}{2\pi a}, \quad (7)$$

where a is the radius of the aperture. We refer to this situation as the “unmodified lens” (UL).

By modifying the aforementioned 2D polynomial method [13], we can place zero rings, rather than vortices, in the PSF at any desired radii. Instead of using the polynomial of Eq. (1), we define h as

$$h(\mathbf{r}_I) := \prod_{n=1}^N \left(|\mathbf{r}_I|^2 - r_n^2 \right). \quad (8)$$

This will produce N zero rings in the PSF, with the n th ring having radius r_n . If at least one ring has a radius smaller than Δ_{UL} , then, by the Rayleigh criterion, we expect that the SOL will have a resolution superior to the UL.

It is to be noted in Eq. (8) that each zero is associated with a quadratic term, in contrast with Eq. (1). This is required to achieve the proper relationship between Fourier transforms and polynomials in polar coordinates. For example, the Fourier transform of the product of a function $t(\mathbf{r}_I)$ with $|\mathbf{r}_I|^2$ roughly follows the rule

$$\mathcal{F} \left\{ |\mathbf{r}_I|^2 t(\mathbf{r}_I) \right\} = \mathcal{F} \left\{ (x_I^2 + y_I^2) t(\mathbf{r}_I) \right\} \rightarrow \left(\frac{\partial^2}{\partial x_L^2} + \frac{\partial^2}{\partial y_L^2} \right) \tilde{t}(\mathbf{r}_L). \quad (9)$$

There is not, however, such a simple derivative rule for the product of $t(\mathbf{r}_I)$ and $|\mathbf{r}_I| = \sqrt{x_I^2 + y_I^2}$.

The complete process for designing a SOL by this method is as follows. First, we choose a band limited transmission function $t(\mathbf{r}_L)$. For a point object at a point \mathbf{r}_o , calculate the Fourier transform $\tilde{t}(\mathbf{r}_I)$ of the transmission function, which is proportional to a (unmodified) PSF $U_I(\mathbf{r}_I)$. (We neglect the function $\gamma(\mathbf{r}_I, \mathbf{r}_o)$, which only modifies the phase of the PSF and provides an overall scaling factor.) We now define a polynomial $h(\mathbf{r}_I)$ using Eq. (8), with at least one $r_n < \Delta_{UL}$. The choice of the r_n values is completely arbitrary, so they can be made *arbitrarily small*. In principle, the lower limits on resolution using this method are determined only by the limits of validity of Fourier optics and by sidelobe tradeoffs we will discuss near the end of the Letter. Next, we multiply $\tilde{t}(\mathbf{r}_I)$ and $h(\mathbf{r}_I)$ to yield a modified transform $\tilde{s}(\mathbf{r}_I) := h(\mathbf{r}_I) \tilde{t}(\mathbf{r}_I)$. This modified function is proportional to the superresolution PSF generated by a new transmission function $t'(\mathbf{r}_L)$. This new transmission function is the transmission needed by the mask in order to produce the new PSF; it can be found by inverse Fourier transforming the modified PSF:

$$t'(\mathbf{r}_L) := \mathcal{F}^{-1} \left\{ \tilde{s}(\mathbf{r}_I) \right\}. \quad (10)$$

With this new transmission function, the basic design process is complete.

Before moving on to an example, it is worth mentioning a few things about our method. First, due to the quadratic terms in Eq. (8), each added zero contributes two derivatives to the Fourier transform. To introduce N zero rings, we thus require that the base transmission function $t(\mathbf{r}_L)$ have its first $2N - 1$ derivatives be continuous, rather than just the first $N - 1$.

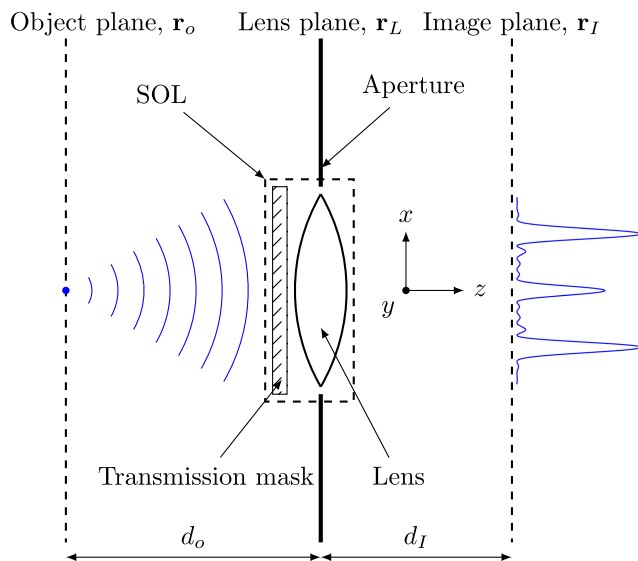


Fig. 1. Proposed superoscillatory lens setup.

Second, the lens shown in Fig. 1 is not strictly necessary, as the quadratic phase imparted by the lens can be incorporated directly into the mask design. Conceptually, though, thinking of the lens as a separate entity allows us to easily analyze the performance of the SOL by comparing it against the UL.

We now design an SOL with our method. The physical parameters used in our simulation are shown in Table 1. The lens radius and focal length were taken from a lens in a company catalog. The object and image distances were chosen to yield a magnification of 1/4, common in nanolithography. The wavelength chosen was one of the smallest operating wavelengths (and hence smallest Δ_{UL}) of the lens.

Next, we need to choose an initial transmission function for the lens. For a standard UL, the transmission function is

$$t(\mathbf{r}_L) := \begin{cases} 1 & |\mathbf{r}_L| \leq a \\ 0 & \text{otherwise} \end{cases} \quad (11)$$

We would like a transmission function that supports $N = 5$ added zeros, which requires that it possess at least $2N - 1$ continuous derivatives. Following our previous work [13], we take our initial transmission function to be

$$t(\mathbf{r}_L) := \begin{cases} \cos^{10}\left(\frac{\pi r_L}{2a}\right) & |\mathbf{r}_L| \leq a \\ 0 & \text{otherwise} \end{cases} \quad (12)$$

We note that a $\cos^n()$ function band limited to its first zero, as in Eq. (12), has n continuous derivatives, so this transmission function can support up to $N = 5$ added zeros.

The PSF intensity of this transmission function is shown in Fig. 2(a). We have indicated the first zero ring of the UL, Δ_{UL} , with a dotted line. To make a superresolution lens, we require that at least one of our r_n be less than Δ_{UL} , which is about 600 nm for this lens. Here, we take $r_1 = 500$ nm; the new PSF intensity is shown in Fig. 2(b). Although we now have superresolution, we can see that there are large sidelobes nearly three times the magnitude of the central lobe. Such sidelobes are an unavoidable feature in superoscillatory functions, and they can severely limit the viewing area of an image.

We can add zero rings to push these sidelobes further away from the desired superresolved imaging spot. The peak of the sidelobes are at about $|\mathbf{r}_L| = 1225$ nm. Figure 2(c) shows the PSF with a second zero ring added at $r_2 = 1370$ nm. We explain the choice of 1370 nm instead of 1225 nm in the following paragraph. We now see that the large sidelobes in Fig. 2(b) have been split into two significantly smaller sidelobes, each only about half the intensity of the central lobe. This is a significant improvement, but we can go further by adding more zero rings near the peaks of these two sidelobes. In Fig. 2(d), we have added two more zero rings, $r_3 = 900$ nm and $r_4 = 1900$ nm. Here, we now have lobes centered at $|\mathbf{r}_L| \approx 2400$ nm that are a little taller than the central lobe (about 1.4 times the intensity), but there is a wide region of low intensity around the central lobe. This final result gives us superresolution with a viewing area of radius

Table 1. Parameters of the Simulated Lens Setup

Lens radius a	0.635 cm
Focal length f	13 mm
Object distance d_o	65 mm
Image distance d_I	16.25 mm
Light wavelength λ_0	385 nm
First zero ring radius Δ_{UL}	603 nm

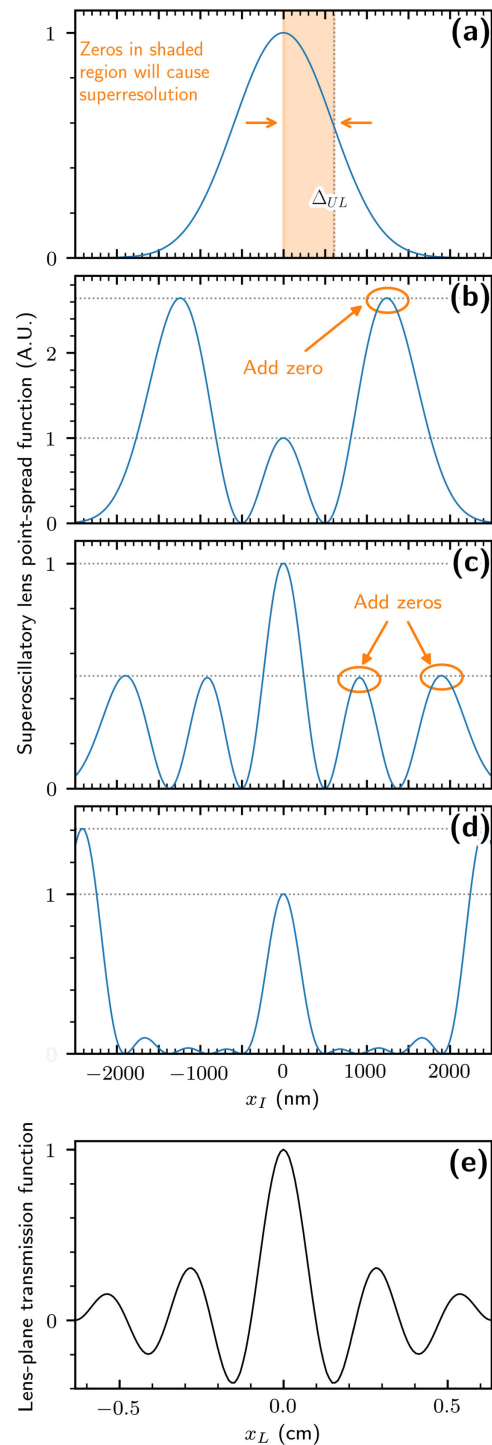


Fig. 2. Designing a superresolution lens. The dotted gray lines are guides to the eye. (a) PSF of the $\cos^{10}()$ transmission function: $\Delta_{UL} \approx 600$ nm. (b) A zero ring has been added with a radius of 500 nm. (c) Another zero ring has been added with a radius of 1370 nm. (d) Two more zero rings have been added with radii of 900 nm and 1900 nm. (e) The lens-plane transmission function needed to produce the PSF in (d).

2000 nm. We note that a limited viewing area is a common issue for SOLs, typically requiring a scanning confocal setup for use [8]. Finally, Fig. 2(e) shows the lens plane transmission function

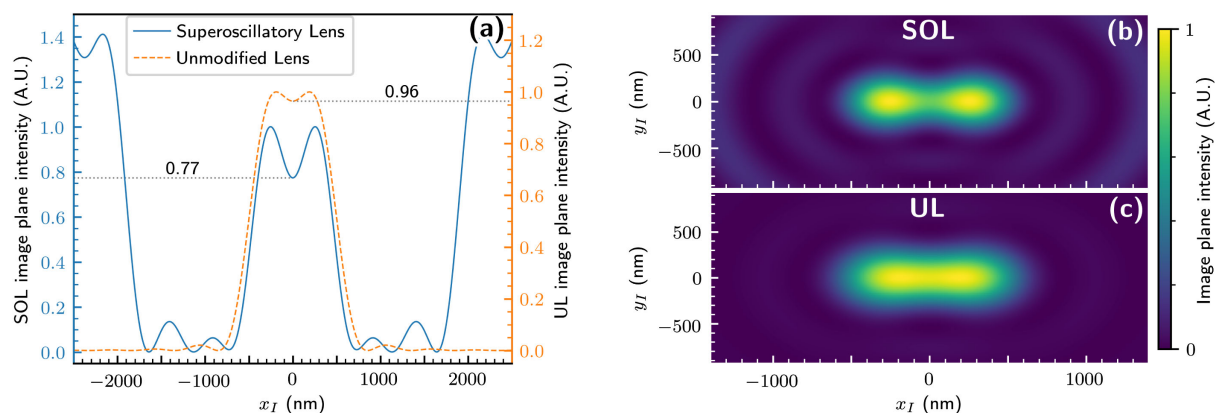


Fig. 3. Combined image of two point sources of incoherent light. (a) x axis view of the combined image for both the SOL and the unmodified lens (UL). (b) Two-dimensional view of the SOL image plane. (c) Two-dimensional view of the UL image plane.

$t'(\mathbf{r}_l)$ that will produce the PSF in Fig. 2(d). Values below zero imply a phase shift of π ; the resultant transmission mask is therefore primarily an amplitude mask, with simple phase flips. These flips are required to create the destructive interference that results in zero rings.

Our choice to set r_2 to 1370 nm instead of 1225 nm was part of the balancing act that this method requires. Setting r_2 to 1225 nm also splits the large sidelobe into smaller lobes, as in Fig. 2(c), except that they do not have equal intensities. Then, setting r_3 and r_4 to the peaks of those lobes results in a PSF similar to that shown in Fig. 2(d), except that the viewing area is slightly smaller, and the large lobes on the end are now four times the intensity of the central lobe, instead of 1.4 times, as in Fig. 2(d). This arises because the zeros have been packed closer together. As is typical in superoscillation, as the zeros get closer together, the sidelobes get larger. Obtaining superresolution with this method thus consists of finding a balance between the central lobe width, viewing area size, and sidelobe intensity; this balance will depend on the specific application. Another factor to consider is absolute intensity, as the central lobes of all the PSFs in Fig. 2 have a maximum intensity that is less than 0.5% of the maximum intensity of the central lobe of the UL PSF. This low intensity is a factor of the number of zeros and their spacing: improving central lobe intensity will typically involve fewer zeros and lower resolution.

Let us now compare the performance of the SOL and the UL. Recall that we set r_1 , the first zero for the SOL, to 500 nm. Following the Rayleigh criterion, if we have achieved superresolution with the SOL, then a pair of point source PSFs placed 500 nm apart should be resolvable with the SOL, but not with the UL. We plot this in Fig. 3, for both the SOL and the UL, assuming incoherent illumination. Figure 3(a) shows an x axis slice of both of the combined images. We can see that for the SOL the two objects are resolvable, with the valley between the central peaks being 77% of the intensity of the peaks, whereas the valley for the UL is about 96% of the value of the central peaks and is thus barely resolvable, if at all. In Figs. 3(b) and 3(c), we show 2D color plots of the combined images for the SOL and UL, respectively.

In this Letter, we have theoretically demonstrated a method to design superresolution lenses that allows for easy positioning of zeros in the image. Here we have used both amplitude and phase modulation; one avenue of future research would be to modify the transmission function to be phase only, which should reduce the loss of intensity and be easier to manufacture. Strategies for constructing phase-only masks from transmission masks have been used before for the detection of vortex beams [14].

Funding. Air Force Office of Scientific Research (FA9550-16-1-0240).

Disclosures. The authors declare no conflicts of interest.

REFERENCES

1. B. R. Frieden, *Opt. Acta* **16**, 795 (1969).
2. B. R. Frieden, *Appl. Opt.* **9**, 2489 (1970).
3. M. G. L. Gustafsson, *J. Microsc.* **198**, 82 (2000).
4. L. Novotny and B. Hecht, *Principles of Nano-Optics*, 2nd ed. (Cambridge University, 2012).
5. M. Berry, in *Quantum Coherence and Reality: In Celebration of the 60th Birthday of Yakir Aharonov*, J. S. Anandan and J. L. Safko, eds. (World Scientific, 1994), pp. 55–65.
6. G. Gbur, *Nanophotonics* **8**, 205 (2018).
7. F. M. Huang and N. I. Zheludev, *Nano Lett.* **9**, 1249 (2009).
8. E. T. F. Rogers, J. Lindberg, T. Roy, S. Savo, J. E. Chad, M. R. Dennis, and N. I. Zheludev, *Nat. Mater.* **11**, 432 (2012).
9. M. Mazilu, J. Baumgartl, S. Kosmeier, and K. Dholakia, *Opt. Express* **19**, 933 (2011).
10. G. H. Yuan, E. T. Rogers, and N. I. Zheludev, *Light Sci. Appl.* **6**, e17036 (2017).
11. A. M. H. Wong and G. V. Eleftheriades, *IEEE Trans. Antennas Propag.* **59**, 4766 (2011).
12. I. Chremmos and G. Fikioris, *J. Phys. A* **48**, 265204 (2015).
13. M. K. S. Smith and G. J. Gbur, *Opt. Lett.* **41**, 4979 (2016).
14. M. Golub, S. Karpeev, N. Kazanskii, A. Mirzov, I. Sisakyan, and V. Soifer, *Sov. J. Quantum Electron.* **18**, 392 (1988).